The reaction mixture was stirred for 15 min and then the solvent removed under vacuum. The residue was extracted with 15 mL of benzene, filtered, and concentrated under vacuum and hexane added to precipitate **10b** as a bright yellow solid, which was collected by filtration, washed with hexane, and dried under vacuum. Yield: 0.036 g, 62%. Anal. Calcd for $C_{36}H_{43}ClNO_2P_2PtRe$: C, 43.22; H, 4.33; N, 1.40. Found: C, 42.54; H, 4.12; N, 1.36.

Reactions of 10b with $AgBF_4$ and $NaBPh_4$. (i) $NaBPh_4$ (0.048 g) was added to **10b** (0.110 g) dissolved in 10 mL of acetone. Solvent was removed under vacuum. The residue was dried under vacuum for 10 min and dissolved in 10 mL of CH_2Cl_2, and the solution was monitored by IR spectroscopy.

(ii) **10b** (0.120 g) was dissolved in 10 mL of CH_2Cl_2. Excess $AgBF_4$ was added and the reaction stirred for 30 min. After filtration, the solvent was removed under vacuum and the residue redissolved in CD_2Cl_2 for ^1H and ^{31}P NMR spectroscopy.

X-ray Crystallography. The BPh_4^- salts of **8b** and **9b** gave poor-quality crystals. Crystals of the BF_4^- salt of **8b** were grown by slow diffusion of hexane into a CH_2Cl_2 solution. Crystals of the BF_4^- salt of **9b** rapidly lost solvent of crystallization. However the PF_6^- salt proved to be more stable to solvent loss and crystals were sealed in 0.2–0.3-mm Lindemann capillaries with a small amount of mother liquor. Anion exchange was carried out by addition of a CH_2Cl_2 solution of $[Et_4N]BF_4$ or $[Et_4N]PF_6$ to a CH_2Cl_2 solution of the BPh_4^- salt of **8b** and **9b**. Precipitation of $[Et_4N]BPh_4$, which is sparingly soluble in CH_2Cl_2, followed by filtration gave a solution with the desired counterion from which suitable crystals were obtained. Relevant experimental details are summarized in Table III. Final atomic positional parameters and complete listings of bond lengths and bond angles have been deposited.

Calculations of van der Waals repulsion energies in the region between the μ-PCy_2, NO, and η^5-C_5H_5 ligands of **8b** were carried out by using the CHEM-X program (Chemical Design Ltd., Oxford, U.K.) following the approach of Orpen for the indirect location of hydride ligands in metal clusters.[25] The program uses a Buckingham potential of the form

$$V(r) = \frac{a \exp(-br)}{r^d} - \frac{c}{r^6}$$

The parameters a–d for various atoms are those reported by Orpen. The Re–H bond length was fixed at 1.6 Å, and positional parameters for the non-hydrogen atoms were taken from the X-ray structural data for **8b**. The hydrogen atoms were positioned by the program with C–H bond lengths of 1.00 Å. Computation of energy maps in the RePPt plane and at positions ±5 and ±10° out of this plane indicated a distinct energy minimum suitable for the location of a hydride ligand close to or in the RePPt plane (±0.2 Å) with a ∠PReH of 70–75°.

EHMO calculations were carried out on the simplified complex $[\eta^5$-$Cp(ON)Re(\mu$-$PH_2)Pt(PH_3)_2]$ with non-hydrogen interatomic distances based on the X-ray crystal structures of **8b** and **9b** with P–H = 1.40 Å and ∠Pt–P–H = 110°. Values for H_{ii} and orbital exponents were taken from ref 37.

Acknowledgment. We are grateful to the Natural Sciences and Engineering Research Council of Canada for financial support of this research.

Registry No. (**6a**)BF_4, 123125-34-8; (**6b**)BF_4, 123125-39-3; (**6b**)BPh_4, 123125-36-0; (**6c**)BF_4, 123125-40-6; (**6c**)BPh_4, 123125-38-2; (**7a**)BF_4, 123125-51-9; (**7b**)BPh_4, 123166-12-1; (**7c**)BPh_4, 123125-53-1; (**8a**)BF_4, 123125-55-3; (**8b**)BF_4, 123125-47-3; (**8b**)BF_4·CH_2Cl_2, 123125-48-4; (**8b**)BPh_4, 123125-41-7; (**8c**)BPh_4, 123125-57-5; (**9a**)BF_4, 101332-90-5; (**9b**)BPh_4, 123125-42-8; (**9b**)PF_6, 123125-45-1; (**9b**)PF_6·2.5CH_2Cl_2, 123125-46-2; (**9c**)BPh_4, 123125-44-0; **10b**, 101307-86-2; (**11b**)BPh_4, 123166-13-2; (**12b**)BPh_4, 123166-14-3; (**13b**)BPh_4, 123166-15-4; **14b**, 123125-62-2; **15b**, 101923-29-9; (**16b**)BPh_4, 123125-59-7; (**17b**)BPh_4, 123125-61-1; $[(\eta^5$-$Cp)Re(CO)(NO)(MeCN)]BF_4$, 92269-93-7; PPh_2H, 829-85-6; PCy_2H, 829-84-5; P^nPr_2H, 19357-87-0; $Pt(C_2H_4)(PPh_3)_2$, 12120-15-9; $Pt(PPh_3)_4$, 14221-02-4; $Pt(C_2H_4)_2(PCy_3)$, 57158-83-5; $[\eta^5$-$Cp(ON)Re(\mu$-$PH_2)Pt(PH_3)_2]$, 123125-49-5; $Pt(CO)_2(PPh_3)_2$, 15377-00-1.

Supplementary Material Available: Examples of first-order rate plots [ln $(A - A_\infty)$ vs t] and plots of spectroscopic changes, ν(NO) region, for the Cl^--catalyzed **8b** to **9b** isomerization and, for compounds (**8b**)BF_4, (**9a**)BF_4, and (**9b**)PF_6, tables of structure determination data, positional and thermal parameters, and complete bond lengths and bond angles (30 pages); tables of final structure factor amplitudes (87 pages). Ordering information is given on any current masthead page.

(37) Summerville, R. H.; Hoffmann, R. *J. Am. Chem. Soc.* **1976**, *98*, 7240.

Contribution from the Department of Chemistry,
University of Toronto, Toronto, Ontario, Canada M5S 1A1

Synthesis of "$PtRu_2$" and "$PtRu_3$" Heterometallic Complexes from the Reaction of $Ru_3(CO)_{11}(PPh_2H)$ with Zerovalent Complexes of Platinum. Single-Crystal X-ray Diffraction Studies of $PtRu_2(\mu$-$PPh_2)(\mu$-$H)(CO)_7(PCy_3)$ and $PtRu_3(\mu$-$PPh_2)(\mu$-$H)(CO)_9(PCy_3)$

John Powell,* John C. Brewer, Giulia Gulia, and Jeffery F. Sawyer

Received November 30, 1988

The reaction of $Ru_3(CO)_{11}(PPh_2H)$ (**4**) with $Pt(C_2H_4)(PPh_3)_2$ gives $PtRu_2(\mu$-$PPh_2)(\mu$-$H)(CO)_7(PPh_3)$ (**6a**) and $Pt_2Ru(CO)_5(PPh_3)_3$ (**7**) as the major products. The reaction of **4** with $Pt(C_2H_4)_2(PCy_3)$ gives $PtRu_2(\mu$-$PPh_2)(\mu$-$H)(CO)_7(PCy_3)$ (**6b**) and $PtRu_3(\mu$-$PPh_2)(\mu$-$H)(CO)_9(PCy_3)$ (**8**) as the major products together with several minor "Ru_xPt_y" species. The molecular structures of **6b** and **8** have been determined by single-crystal X-ray diffraction. Crystal data for **6b**: $C_{37}H_{44}O_7P_2PtRu_2$ crystallizes in space group $P2_1/n$ with a = 13.075 (5) Å, b 20.576 (4) Å, c = 15.316 (7) Å, β = 102.38 (3)°, V = 4025 Å^3, and D_x = 1.75 g cm^{-3} for Z = 4; R (R_w) = 0.0324 (0.0327) for 5932 observed data [$I \geq 3\sigma(I)$]. Crystal data for **8**: $C_{45}H_{56}O_9P_2PtRu_3$·CH_2Cl_2 crystallizes in space group $P2_1/c$ with a = 9.605 (3) Å, b = 23.713 (12) Å, c = 20.600 (5) Å, β = 95.76 (2)°, V = 4668 Å^3, and D_x = 1.77 g cm^{-3} for Z = 4; R (R_w) = 0.0605 (0.0645) for 3954 observed data [$I \geq 3\sigma(I)$]. Complex **6b** contains a $PtRu_2$ triangle with one direct PtRu and one direct RuRu metal–metal bond. The hydride bridges a PtRu edge while the μ-PPh_2 ligand bridges the RuRu edge such that the RuPRu plane is approximately orthogonal to the $PtRu_2$ plane. The structure of **8** is formally derived from that of **6b** by the addition of a "$Ru(CO)_2$" moiety to **6b** along a line bisecting the Ru–Ru bond and passing through P_μ of the PPh_2 group such that the resulting structure essentially consists of a square-planar $(Cy_3P)(OC)Pt(H)(Ru2)$ center linked by the μ-H and Pt–Ru2 metal–metal bonds to a $Ru_3(\mu$-$CO)_2(\mu$-$PPh_2)(CO)_6$ planar moiety. In **6b**, the bridging hydrogen atom was located and refined such that Pt–H_μ = 1.65 (4) Å, Ru1–H_μ = 1.66 (4) Å, and PtH_μRu1 = 121 (3)°.

Introduction

The oxidative addition of the P–H bond of a secondary phosphine complex to zerovalent phosphine complexes of platinum is a simple and effective means of incorporating a single bridging-phosphido group into a range of "MPt", "MPt_2", and "MPt_3" complexes.[1-5] Typically, complexes of the type $(OC)_xM(PR_2H)$ (M = Cr, Mo, W, x = 5; M = Fe, Ru, x = 4)[1,4] and cationic

(1) Powell, J.; Gregg, M. R.; Sawyer, J. F. *J. Chem. Soc., Chem. Commun.* **1984**, 1149.

0020-1669/89/1328-4470$01.50/0

Table I. ^1H and $^{31}P\{^1H\}$ NMR Data (δ, ppm; J, Hz) for Complexes **6a**, **6b**, and **8**, Recorded in CD_2Cl_2

	$PtRu_3(\mu\text{-}PPh_2)(\mu\text{-}H)(CO)_9(PCy_3)$ (**8**)	$PtRu_2(\mu\text{-}PPh_2)(\mu\text{-}H)(CO)_7(PR_3)$	
		6b ($PR_3 = PCy_3$)	**6a** ($PR_3 = PPh_3$)
$\delta(H)$	−10.2	−11.1	−10.5
$^1J_{^{195}Pt-^1H}$	570	534	540
$^2J_{^{31}P-^1H}$	11.7, 8.5	14.3, 10.5	18, 11
$\delta(P_\mu)$	387	155	153
$^1J_{^{195}Pt-^{31}P_\mu}$	202	179	199
$\delta(PC_3)$	66	52	32.5
$^1J_{^{195}Pt-^{31}P}$	2587	2773	2879
$^3J_{^{31}P-^{31}P_\mu}$	10	13	15

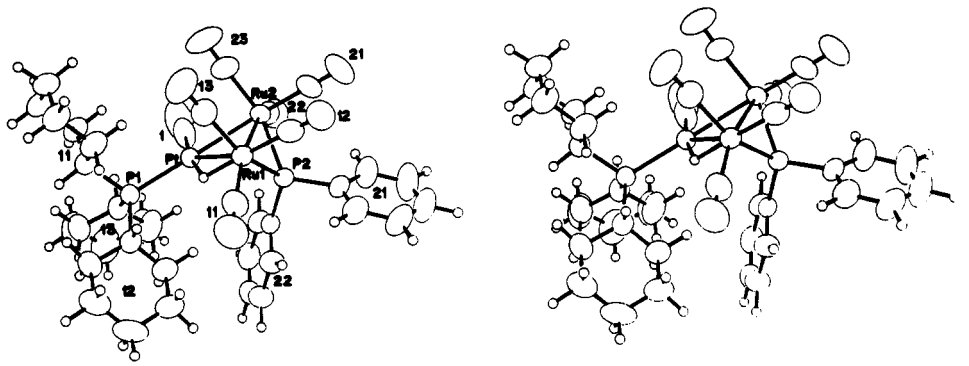

Figure 1. Molecular structure of $PtRu_2(\mu\text{-}PPh_2)(\mu\text{-}H)(CO)_7(PCy_3)$ (**6b**).

complexes such as $[Cp(OC)_xM(PR_2H)]^+$ (M = Mo, W, x = 3; M = Fe, Ru, x = 2)[2,3] and $[Cp(OC)(ON)Re(PR_2H)]^+$ have sufficiently acidic P–H bonds to undergo such reactions. Spectroscopic studies of these systems have provided considerable insight into "platinum-assisted" CO labilization at 18-electron metal centers, hydrogen-transfer processes between the different metal sites, and cluster assembly pathways in "MPt_x" systems. Provided that the required monosubstituted secondary-phosphine carbonyl complex $M_y(CO)_z(PR_2H)$ is synthetically accessible, the approach may be extended to the synthesis and study of "M_yPt_x" phosphido-bridged systems. We have recently reported that the complex $Re_2(CO)_9(PR_2H)$ reacts with $Pt(C_2H_4)(PPh_3)_2$ and $Pt(C_2H_4)_2(PCy_3)$ in CH_2Cl_2 at 20 °C, to give $PtRe_2(\mu\text{-}PR_2)(\mu\text{-}H)(CO)_8(PPh_3)$ (**1a**) and $PtRe_2(\mu\text{-}PR_2)(\mu\text{-}H)(CO)_9(PCy_3)$ (**2**), respectively.[6] Complex **2** has a relatively short lifetime in solution

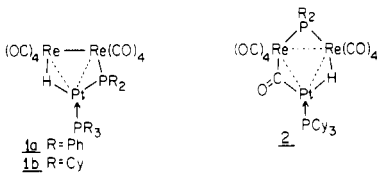

and disproportionates to $Re_2(\mu\text{-}PR_2)(\mu\text{-}H)(CO)_8$ (**3**) and $Pt_3(CO)_3(PCy_3)_3$. The hydrido- and phosphido-bridged product **3** will react further with a second equivalent of $Pt(C_2H_4)_2(PCy_3)$ to give $PtRe_2(\mu\text{-}PR_2)(\mu\text{-}H)(CO)_8(PCy_3)$ (**1b**). Unusual features of these reactions are (i) the platinum-assisted labilization of CO loss from Re in the formation of **1** and **3** under room-temperature conditions [N.B. formation of $Re_2(\mu\text{-}PR_2)(\mu\text{-}H)(CO)_8$ directly from $Re_2(CO)_9(PR_2H)$ by thermal CO loss requires temperatures >170 °C[6]]; (ii) the difference in the location of the phosphido bridge [Re(μ-PR_2)Pt in **1**; Re(μ-PR_2)Re in **2**], which is possibly a consequence of kinetic selection in the formation of **2**; and (iii) the lability of the μ-PR_2 ligand with regard to intramolecular "Re(μ-PR_2)Re" ⇄ "Re(μ-PR_2)Pt" rearrangements [e.g. formation of **2**, and the formation of **1b** from $Re_2(\mu\text{-}PR_2)(\mu\text{-}H)(CO)_8$ and $Pt(C_2H_4)_2(PCy_3)$]. In this paper, we report the results pertaining to the reactions of $Ru_3(CO)_{11}(PPh_2H)$[7] (**4**) and $Ru_3(CO)_{10}(\mu\text{-}H)(\mu\text{-}PPh_2)$[7] (**5**) with $Pt(C_2H_4)(PPh_3)_2$ and $Pt(C_2H_4)_2(PCy_3)$, which give rise to $PtRu_2(\mu\text{-}PPh_2)(\mu\text{-}H)(CO)_7(PR_3)$ (**6**) [**6a**, PR_3 = PPh_3; **6b**, PR_3 = PCy_3] and $PtRu_3(\mu\text{-}PPh_2)(\mu\text{-}H)(\mu\text{-}CO)_2(CO)_7(PCy_3)$ (**8**) as major products. The structures of **6b** and **8** have been determined by single-crystal X-ray diffraction studies.

Results

The synthesis of the monosubstituted diphenylphosphine complex $Ru_3(CO)_{11}(PPh_2H)$ (**4**) has been reported by Carty et al.[7] following the procedure initially described by Bruce et al.[8] for the synthesis of $Ru_3(CO)_{11}(PMe_2Ph)$ in which CO labilization is effected by the use of radical initiators (eq 1). Kaesz et al.[9]

$$Ru_3(CO)_{12} + PR_3 \xrightarrow[THF]{Na^+Ph_2CO^-} \underset{\mathbf{4}}{Ru_3(CO)_{11}(PR_3)} \qquad (1)$$

$PR_3 = PPh_2H$

recently reported that monosubstitution of $Ru_3(CO)_{12}$ could be effected by the addition of acetate ion. This reaction can also be used to synthesize $Ru_3(CO)_{11}(PPh_2H)$, but the acetate also promotes further decarbonylation to give the internal oxidative-addition product $Ru_3(\mu\text{-}PPh_2)(\mu\text{-}H)(CO)_{10}$ (**5**) (eq 2). As such, the procedure of Carty (eq 1) is the preferred method for the synthesis of $Ru_3(CO)_{11}(PPh_2H)$.

$$Ru_3(CO)_{12} + PPh_2H \xrightarrow[25°C,\ THF]{[PPN][OAc]} \underset{\mathbf{4}}{Ru_3(CO)_{11}(PPh_2H)} \xrightarrow{[PPN][OAc]} \underset{\mathbf{5}}{Ru_3(\mu\text{-}H)(\mu\text{-}PPh_2)(CO)_{10}} \qquad (2)$$

The reaction of $Ru_3(CO)_{11}(PPh_2H)$ with $Pt(C_2H_4)(PPh_3)_2$ in CD_2Cl_2 at 20 °C (NMR monitoring) occurs as outlined in eq 3. The major phosphido-bridged species is $PtRu_2(\mu\text{-}PPh_2)(\mu\text{-}H)(CO)_7(PPh_3)$ (**6a**) in which the phosphido ligand bridges the two ruthenium atoms. The structure of **6a** is based on ^1H and $^{31}P\{^1H\}$ NMR data (see Table I and later discussion) and an X-ray

(2) Powell, J.; Sawyer, J. F.; Smith, S. J. *J. Chem. Soc., Chem. Commun.* **1985**, 1312.
(3) Powell, J.; Sawyer, J. F.; Stainer, M. V. R. *J. Chem. Soc., Chem. Commun.* **1985**, 1314.
(4) Powell, J.; Gregg, M. R.; Sawyer, J. F. *J. Chem. Soc., Chem. Commun.* **1987**, 1029.
(5) Powell, J.; Gregg, M. R.; Sawyer, J. F. *Inorg. Chem.* **1988**, *27*, 4521.
(6) Powell, J.; Brewer, J. C.; Gulia, G.; Sawyer, J. F. *Inorg. Chem.*, submitted for publication.
(7) MacLaughlin, S. A.; Taylor, N. J.; Carty, A. J. *Organometallics* **1984**, *3*, 392.
(8) Bruce, M. I.; Matisons, J. G.; Nicholson, B. K. *J. Organomet. Chem.* **1983**, *247*, 321.
(9) Lavigne, G.; Kaesz, H. D. *J. Am. Chem. Soc.* **1986**, *106*, 4647.

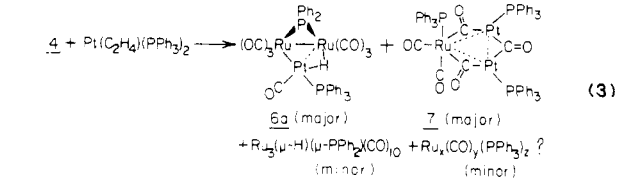

(3)

diffraction study of a PCy_3 analogue (Figure 1). Formation of **6a** from $Ru_3(CO)_{11}(PPh_2H)$ necessitates loss of a "$Ru(CO)_4$" fragment from **4**. This could lead to formation of $Ru_3(CO)_{12}$, which has been previously shown to react with $Pt(stilbene)(PPh_3)_2$ to give the complex $PtRu_2(CO)_5(PPh_3)_3$ (**7**).[10] Complex **7** is also obtained as one of the major products of eq 3. Contrary to the early report in which $Ru_3(CO)_{12}$ and $Pt(stilbene)(PPh_3)_2$ were allowed to react for 5 days,[10] we have found that reaction of $Ru_3(CO)_{12}$ with $Pt(C_2H_4)(PPh_3)_2$ proceeds quickly with very significant amounts of **7** being formed within 5 min of mixing. The formation of **7** in eq 3 is readily confirmed by comparison of the $^{31}P\{^1H\}$ NMR spectrum of the reaction mixture with that of an authentic sample of **7**.

The reaction of $Ru_3(\mu\text{-}PPh_2)(\mu\text{-}H)(CO)_{10}$ (**5**) with $Pt(C_2H_4)(PPh_3)_2$ (eq 4) proceeds more slowly than the reaction of **4** with $Pt(C_2H_4)(PPh_3)_2$ (eq 3) but likewise gives **6a** as the major

$$\mathbf{5} + Pt(C_2H_4)(PPh_3)_2 \rightarrow \mathbf{6a} + \text{unidentified } Ru_x(CO)_y(PPh_3)_z \text{ products} \quad (4)$$

product. Besides the resonances assignable to **6a**, the $^{31}P\{^1H\}$NMR spectrum of the mixture of reaction products contained unidentified singlet resonances at 48, 30, and 16 ppm which, given that formation of **6a** from **5** involves loss of a "$Ru(CO)_3$" fragment, may be due to $Ru_3(CO)_9(PPh_3)_3$, $Ru(CO)_3(PPh_3)_2$, and/or other PPh_3-substituted ruthenium carbonyl complexes. No resonances assignable to **7** were observed in this reaction.

The reaction of $Ru_3(CO)_{11}(PPh_2H)$ with $Pt(C_2H_4)_2(PCy_3)$ (eq 5) is more complex than its reaction with $Pt(C_2H_4)(PPh_3)_2$ (eq 3). Upon addition of a molar equivalent of $Pt(C_2H_4)_2(PCy_3)$ to

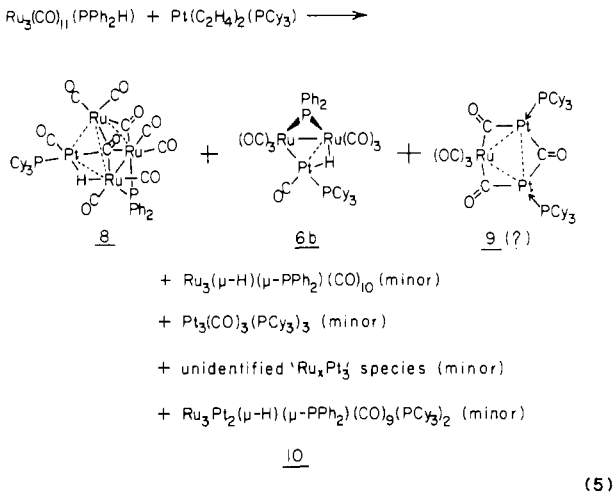

(5)

4 in CD_2Cl_2 (NMR monitoring of the reaction), $PtRu_3(\mu\text{-}PPh_2)(\mu\text{-}H)(CO)_9(PCy_3)$ (**8**) and $PtRu_2(\mu\text{-}PPh_2)(\mu\text{-}H)(CO)_7(PCy_3)$ (**6b**) are obtained in a ca. 2:1 ratio (eq 5; >90% reaction after 90 min, 20 °C). The complexes **8** and **6b** together with a small amount of $Ru_3(\mu\text{-}PPh_2)(\mu\text{-}H)(CO)_{10}$ (**5**) and a small amount of a complex tentatively formulated as $Ru_3Pt_2(\mu\text{-}PPh_2)(\mu\text{-}H)(CO)_9(PCy_3)_2$ (**10**) are the only μ-H- and μ-PPh_2-containing products. The formation of **6b** requires the loss of a "$Ru(CO)_4$" fragment, which, as noted above, could lead to formation of $Ru_3(CO)_{12}$. Reaction of $Ru_3(CO)_{12}$ with $Pt(C_2H_4)_2(PCy_3)$ could lead to $Pt_2Ru(CO)_6(PCy_3)_2$ (**9**), which is structurally similar to **7**. Although **9** was not isolated, the $^{31}P\{^1H\}$ NMR spectrum of the mixture of the reaction products of eq 5 contained a moderately intense resonance pattern typical of a symmetrical $R_3PPtPtPR_3$ unit (similar to that observed for **7**), which we tentatively assign to **9** (see Experimental Section for NMR data). Minor resonances assignable (i) to **5**, (ii) to $Pt_3(CO)_3(PCy_3)_3$, (iii) to an unidentified but symmetrical $Pt_3Ru_x(CO)_y(PCy_3)_3$ species [possibly $Pt_3Ru(CO)_6(PCy_3)_3$ formed from further reaction of **9** with $Pt(C_2H_4)_2(PCy_3)$], and (iv) to $Pt_2Ru_3(\mu\text{-}PPh_2)(\mu\text{-}H)(CO)_9(PCy_3)_2$ (**10**) [tentative assignment, formed from the reaction of **8** with $Pt(C_2H_4)_2(PCy_3)$] are also observed. The reaction of $Pt(C_2H_4)_2(PCy_3)$ with $Ru_3(\mu\text{-}PPh_2)(\mu\text{-}H)(CO)_{10}$ (**5**) occurs more slowly than reaction with **4** but gives a product distribution similar to that in eq 5.

The μ-hydrido-μ-phosphido complexes **6b** and **8**, the major products of the reaction of **4** or **5** with $Pt(C_2H_4)_2(PCy_3)$, were isolated by fractional crystallization and their molecular structures determined by X-ray diffraction.

Molecular Structures of $PtRu_2(\mu\text{-}PPh_2)(\mu\text{-}H)(CO)_7(PCy_3)$ (6b) and $PtRu_3(\mu\text{-}PPh_2)(\mu\text{-}H)(CO)_9(PCy_3)$ (8). ORTEP drawings and the labeling schemes are given in Figures 1 and 2. Details of the structure determinations, bond lengths, and bond angles are given in Tables II–IV. Complex **6b**, a 46-electron cluster,[11]

Table II. Crystal, Data, Details of Intensity Measurements, and Structure Refinements[a]

compd	$C_{37}H_{44}O_7P_2PtRu_2$ (**6b**)	$C_{45}H_{56}O_9P_2PtRu_3\cdot CH_2Cl_2$ (**8**)
system	monoclinic	monoclinic
a, Å	13.075 (5)	9.605 (3)
b, Å	20.576 (4)	23.713 (12)
c, Å	15.316 (7)	20.600 (5)
β, deg	102.38 (3)	95.76 (2)
V, Å^3	4025	4668
Z	4	4
fw	1059.9	1386.1
space group	$P2_1/n$	$P2_1/c$
T, °C	20	20
λ, Å	0.710 69	0.710 69
ρ_{calcd}, g cm^{-3}	1.75	1.97
μ(Mo K$\bar{\alpha}$), cm^{-1}	43.5	40.7
transm coeff	0.478–0.623	0.547–0.674
$R(F_o^2)$	0.0324	0.0605
$R_w(F_o^2)$	0.0327	0.0645

Table III. Selected Bond Lengths (Å)

compound **6b**		compound **8**	
Pt–Ru1	2.8755 (5)	Pt–Ru1	2.764 (2)
–Ru2	2.7248 (5)	–Ru2	2.846 (2)
–P1	2.332 (2)	–Ru3	2.895 (2)
–C1	1.847 (7)	–P1	2.330 (4)
–H_μ	1.65 (4)	–C1	1.80 (2)
Ru1–Ru2	2.7789 (6)	Ru1–Ru2	2.800 (2)
–P2	2.328 (1)	–Ru3	2.680 (2)
–C11	1.913 (7)	–P2	2.311 (5)
–C12	1.883 (7)	–C3	2.09 (2)
–C13	1.922 (7)	–C11	1.89 (2)
–H_μ	1.66 (4)	–C12	1.88 (2)
Ru2–P2	2.306 (1)	Ru2–Ru3	2.686 (2)
–C21	1.870 (7)	–P2	2.316 (5)
–C22	1.894 (6)	–C2	2.10 (2)
–C23	1.937 (8)	–C21	1.90 (2)
P1–C111	1.863 (5)	–C22	1.86 (2)
–C121	1.858 (6)	Ru3–C2	2.13 (2)
–C131	1.858 (6)	–C3	2.10 (2)
P2–C211	1.823 (6)	–C31	1.85 (2)
–C221	1.830 (6)	–C32	1.90 (2)
C1–O1	1.139 (9)	P1–C111	1.825 (15)
⟨*Cnm–Onm*⟩	1.140 (7)	–C121	1.864 (19)
Pt–P2	3.204 (1)	–C131	1.857 (22)
		P2–C211	1.841 (18)
		–C221	1.807 (17)
		C1–O1	1.18 (3)
		C2–O2	1.17 (3)
		C3–O3	1.18 (3)
		⟨*Cnm–Onm*⟩	1.13 (3)
		Pt–P2	3.327 (5)

(10) Bruce, M. I.; Shaw, G.; Stone, F. G. A. *J. Chem. Soc., Dalton Trans.* **1972**, 1781.

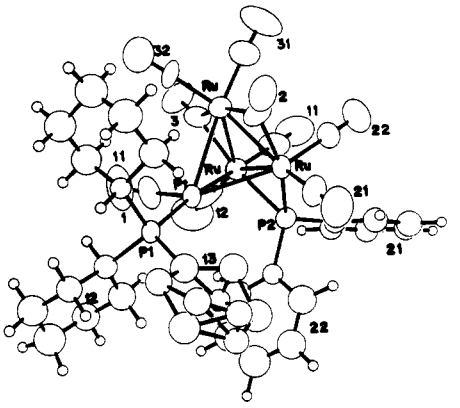

Figure 2. Molecular structure of $PtRu_3(\mu\text{-}PPh_2)(\mu\text{-}H)(CO)_9(PCy_3)$ (**8**).

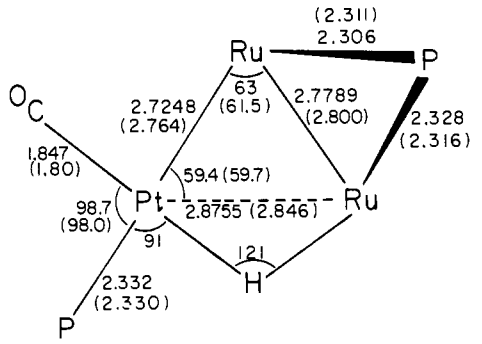

Figure 3. Comparison of the structural features of the "$(OC)(Ph_3P)$-$PtRu_2(\mu\text{-}PPh_2)$" unit of **6b** and **8** (data in parentheses).

consists of a $PtRu_2$ triangle of atoms that is edge-bridged by a hydride atom in the $PtRu_2$ plane and by a diphenylphosphido ligand bridging the Ru–Ru edge such that the Ru_2P plane makes an angle of 84° with the Ru_2Pt plane. Notably, in this arrangement the Pt···P2 distance is 3.204 (1) Å and this weak contact is approximately trans to the P2–C211 bond [∠Pt–P2–C211 = 176.6 (2)°; ∠Pt–P2–C221 = 82.1 (2)°] although the distortions in the ∠RuP2C*n*21 angles are very small. A similar but more pronounced effect has been observed in the structure of (μ-hydrido)(μ-diphenylphosphido)(nonacarbonyltriruthenium where there is a weak Ru2···P interaction [2.779 (1) Å] completing a distorted Ru_3P_μ tetrahedron.[12] The environment of the Pt atom in **6b** is an approximately square plane defined by the bonds Pt–P1, Pt–C1, Pt–Ru2, and Pt–H_μ (see Figure 3). Angles between these bonds are 82.1 (2)–98.7 (2)°, and the trans Ru2PtP1 and C1PtH_μ angles are 178.90 (4) and 170 (1)°, respectively. This interpretation assumes that the Pt–Ru2 edge of the $PtRu_2$ triangle represents a direct M–M bond while the bonding on the Pt–Ru1 edge occurs mainly through the Pt–H_μ and Ru–H_μ bonds. Consistent with this notion, it is notable that the Pt–Ru1 distance [2.8755 (5) Å] is 0.15 Å longer than the Pt–Ru2 distance [2.7248 (5) Å]. Similar trends are observable in **8** (see below). The only other Pt–Ru distances available for comparison are for two Pt_2Ru systems (one of which has been characterized in solvated and unsolvated forms) that however involve carbonyl-bridged Ru–Pt and Pt–Pt edges.[13,14] In these latter structures, the Pt–Ru distances are 2.707 (2)–2.741 (2) Å, comparable to the present Pt–Ru2 distance.

In the Pt–H–Ru bridge of **6b**, the Pt–H and Ru–H distances are 1.65 (4) and 1.66 (4) Å, respectively, and the Pt–H–Ru angle is 121 (3)°. Values of recently determined Pt–H distances have been summarized,[15] and the whole area of crystallographically

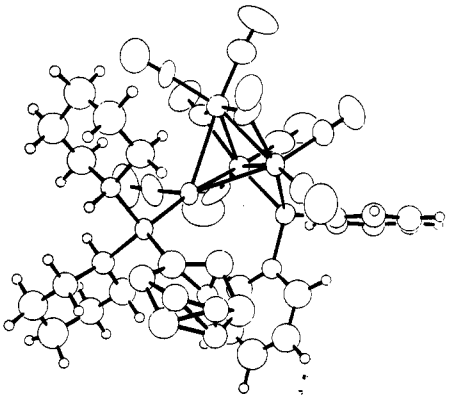

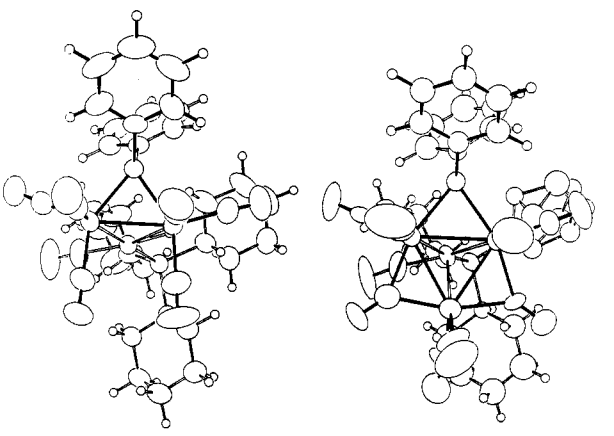

Figure 4. ORTEP drawings of **6b** (left) and **8** (right) in comparable orientations illustrating the very small changes in the structural features of the "$PtRu_2(\mu\text{-}PPh_2)(\mu\text{-}H)(CO)_5$" unit common to both **6b** and **8**.

determined transition-metal hydride complexes has been reviewed.[16] The present values are, however, significantly shorter than the average Pt–H_μ and Ru–H_μ distances quoted by Teller and Bau and are closer to values considered typical of terminal Pt(Ru)–H distances.[16]

The immediate coordination spheres of Ru1 and Ru2 in **6b** are distorted "$RuC_3H_\mu P_\mu$" and "$RuC_3P_\mu Pt$" octahedra, respectively. The most noticeable distortion in this region of the molecule involves a significant bending of the axial carbonyl groups C11–O11 and C22–O22 toward the bridging-diphenylphosphido group [Ru2Ru1C11 and Ru1Ru2C22 bond angles are 159.1 (2) and 152.5 (2)°, respectively], and the torsion angle [C11–Ru1–Ru2–C22] = 18.0 (7)° is significantly larger than those between the eclipsed equatorial CO's ([C12–Ru1–Ru2–C21] = 2.7 (3)°; [C13–Ru1–Ru2–C23] = −1.6 (3)°). This displacement does reduce interactions between the carbonyl on Pt and C22–O22 (τ[C1–Pt–Ru2–C22 = −29.8 (3)°; τ[P1–Pt–Ru1–C11] = 22.9 (2)). The observed Ru–Ru distance [2.7789 (6) Å] is, however, slightly shorter than the Ru–Ru distance in **8** [2.800 (2) Å] and the RuRu distances in $Ru_3(CO)_{12}$[17] (average 2.8542 Å) and the Ru–Ru distance for the (μ-PHPh)(μ-H) edge [2.903 (1) Å] in $Ru_3(\mu\text{-}PHPh)(\mu\text{-}H)(CO)_{10}$ [the other Ru–Ru distances are 2.848 and 2.853 (1) Å[16]].

The structure of **8** can be related to **6b** by the addition of a "$Ru(CO)_2$" moiety to **6b** in a direction between carbonyls 13 and 23 and along a line bisecting the Ru–Ru bond and passing through P2 (Figure 2). The distortions in the arrangements of the peripheral atoms on the phosphines and the planar coordination

(11) Stone, F. G. A. *Inorg. Chim. Acta* **1981**, *50*, 33.
(12) MacLaughlin, S. A.; Carty, A. J.; Taylor, N. J. *Can. J. Chem.* **1982**, *60*, 87.
(13) Modinos, A.; Woodward, P. *J. Chem. Soc., Dalton Trans.* **1975**, 1534.
(14) Bruce, M. I.; Matisons, J. G.; Skelton, B. W.; White, A. H. *Aust. J. Chem.* **1982**, *35*, 687.
(15) Powell, J.; Sawyer, J. F.; Shiralian, M. *Organometallics* **1989**, *8*, 577.
(16) Teller, R. G.; Bau, R. *Struct. Bonding (Berlin)* **1981**, *44*, 1.
(17) Churchill, M. R.; deBoer, B. G. *Inorg. Chem.* **1977**, *16*, 878.
(18) Iwasaki, F.; Mays, M. J.; Raithby, P. R.; Taylor, P. L.; Wheatley, P. J. *J. Organomet. Chem.* **1981**, *213*, 185.

Table IV. Bond Angles (deg)

Compound 6b

At Pt	Ru2	P1	C1	Hμ
Ru1	59.43(1)	119.69(3)	140.9(2)	30(2)
Ru2		178.90(4)	82.1(2)	88(1)
P1			98.7(2)	91(1)
C1				170(1)

At Ru1	Ru2	P2	C11	C12	C13	Hμ
Pt	57.59(1)	75.20(4)	114.8(2)	148.9(2)	86.2(2)	30(1)
Ru2		52.79(4)	159.1(2)	91.8(2)	95.5(2)	86(1)
P2			107.5(2)	90.8(2)	148.2(2)	86(1)
C11				95.8(3)	103.6(3)	85(1)
C12					92.3(3)	176(1)
C13						91(1)

At Ru2	Ru1	P2	C21	C22	C23
Pt	62.99(1)	78.65(4)	163.7(2)	100.0(2)	83.2(2)
Ru1		53.52(3)	101.0(2)	152.5(2)	94.0(2)
P2			94.1(2)	104.0(2)	147.3(2)
C21				95.9(3)	95.9(3)
C22					105.8(3)

At P1	C111	C121	C131
Pt	111.9(2)	112.7(2)	110.3(2)
C111		104.8(2)	105.7(2)
C121			111.2(3)

At P2	Ru1	Ru2	C211	C221
Pt	60.18(3)	56.48(3)	176.6(2)	82.1(2)
Ru1		73.70(4)	119.2(2)	119.6(2)
Ru2			120.2(2)	123.6(2)
C211				100.8(2)

Pt - Hμ - Ru1	121(3)
Pt - C1 - O1	174.7(7)
<Ru - Cnm - Onm>	178.2(10)

Compound 8

At Pt	Ru2	Ru3	P1	C1	At Ru1
Ru1	59.86(5)	56.48(5)	171.4(1)	79.7(6)	Pt
Ru2		55.78(5)	123.6(1)	138.1(6)	Ru2
Ru3			132.1(1)	94.3(6)	Ru3
P1				98.0(6)	P2
					C3
					C11

At Ru1	Ru2	Ru3	P2	C3	C11	C12	C31	C32
Pt	61.54(5)	64.23(5)	81.4(1)	90.2(6)	164.4(8)	101.8(7)	172.8(7)	100.9(7)
Ru2		58.65(6)	52.9(1)	108.8(6)	103.7(8)	151.5(7)	114.9(7)	138.5(8)
Ru3			111.4(1)	50.3(6)	104.7(7)	138.1(6)	113.0(8)	143.3(7)
P2				161.6(6)	93.5(8)	104.4(6)	94.8(10)	99.5(9)
C3					90.3(9)	93.3(9)	92.3(9)	96.4(9)
C11						93.8(10)		86.2(10)

At Ru2	Ru1	Ru3	P2	C2	C21	C22
Pt	58.61(5)	63.03(5)	79.5(1)	86.2(6)	112.8(7)	151.1(7)
Ru1		58.45(5)	52.7(1)	109.4(6)	157.1(7)	94.4(7)
Ru3			111.1(1)	51.0(6)	140.1(7)	95.1(6)
P2				161.4(6)	106.5(7)	92.5(6)
C2					90.0(9)	94.3(8)
C21						96.2(10)

At Ru3	Ru1	Ru2	C2	C3
Pt	59.28(5)	61.19(5)	84.5(5)	86.6(6)
Ru1		62.90(6)	112.9(5)	50.2(6)
Ru2			50.1(5)	112.9(6)
C2				163.0(8)
C3				
C31				

At P1	C111	C121	C131
Pt	109.5(5)	110.0(6)	116.7(7)
C111		105.7(8)	104.6(8)
C121			109.7(9)

At P2	Ru1	Ru2	C211	C221
Pt	55.2(1)	57.3(1)	171.9(6)	85.0(5)
Ru1		74.5(1)	117.4(6)	123.2(6)
Ru2			119.5(6)	119.2(6)
C211				102.7(8)

Pt - C1 - O1	173(2)	Ru1 - C3 - Ru3	79.6(8)
Ru2 - C2 - Ru3	78.9(7)	- O3	144(2)
- O2	143(2)	Ru3 - C3 - O3	136(2)
Ru3 - C2 - O2	138(2)	<Ru - Cnm - Onm>	177(2)

geometry at Pt after this addition are generally very small as can be seen from the results of applying a least-squares fit of parts of the two structures[19] (see also Figures 3 and 4). Thus the C and O atoms of the carbonyls bridging Ru1 and Ru2 and Ru3 deviate by ca. 0.57 and 1.51 Å from their position in **6b** while the maximum deviation between analogous C atom positions in the phenyl and cyclohexyl groups is 0.79 Å.

The complex $PtRu_3(\mu\text{-}PPh_2)(\mu\text{-}H)(CO)_9(PCy_3)$ (**8**) is an example of a 58-electron M_3Pt cluster and, as expected, contains a closed $PtRu_3$ tetrahedron of metals. The basic structural features of **8** are similar to those observed for the 58-electron cluster

(19) By the use of the program BMFIT: Yuen, P. S.; Nyburg, S. C. *J. Appl. Crystallogr.* **1979**, *12*, 258.

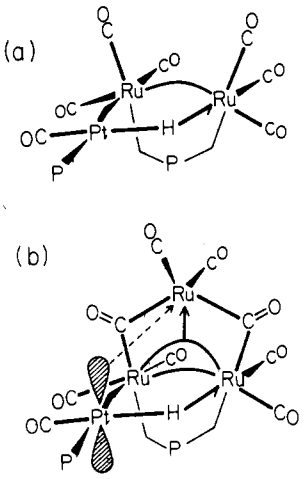

Figure 5. Simplified localized bonding scheme of **6** and **8**.

$Os_3Pt(\mu\text{-}H)_2(CO)_{10}(PCy_3)$.[20] While this latter cluster has all terminal CO's, compound **8** has two μ-CO's and a μ-PPh_2 group bridging Ru–Ru bonds. The bridging hydrogen, which was not directly located, is by analogy with the structures of **6b** and $Os_3Pt(\mu\text{-}H)_2(CO)_{10}(PCy_3)$ inferred to be trans to the C1–O1 group on Pt and bridging the longer of the in-plane Pt–Ru distances. As with **6b** above, a Pt–Ru bond completes a square plane of bonds around Pt. The remaining Pt–Ru3 distance is longer [2.895 (2) Å] than the in-plane Pt–Ru distances and is approximately trans to C31–O31 [Pt–Ru3–C31 = 172.8 (7)°]. Similarly, the Pt···P2 distance [3.327 (5) Å], although weaker than that in **6b**, is again trans to the P2–C211 bond [Pt···P2–C211 = 171.9 (6)° and Pt···P2–C221 = 85.0 (5)°]. Thus, the main bonding interactions in the cluster appear to be between a square-planar Pt atom and a $Ru_3(\mu\text{-}CO)_2(\mu\text{-}PPh_2)$ moiety.[21] The addition of the extra "$Ru3(CO)_2$" fragment across Ru1–Ru2 in **8** slightly lengthens that distance vis-à-vis **6b**, but has virtually no effect on the Ru–P_μ distances and bonding arrangement at Pt (see Figure 3), and the Pt–PCy_3 distances in **6b** and **8** have essentially the same length. Torsion angles τ[C1–Pt–Ru1–C12] = −35.8 (9)° and τ[P1–Pt–Ru2–C21] = 14.6 (7)° do indicate a 6–8° rotation from the values in **6b** above, principally due to distortions in the RuRuC angles for the carbonyls involved, with the changes in angles at Ru1 and Ru2 occurring in opposite directions.

Localized bonding models are particularly successful at rationalizing molecular geometries.[22] The simple bonding schemes shown in Figure 5 are consistent with the observed structural features, with metal valency states of 2 (Pt, Ru1, Ru2) for **6b**, and with valency states of 2 (Pt, Ru3) and 4 (Ru1, Ru2) for **8**. In order to attain an octahedral field at Ru3, in complex **8**, it is necessary to postulate donation of electron density from Pt to Ru3. This interaction must be very weak as the change in the planar coordination of Pt, **6b** vs **8**, is very small. Evidence for a weak Pt→Ru_3 interaction is the increase in the Pt···P_μ separation from 3.204 (1) (**6b**) to 3.327 Å (**8**).

In **6b**, the Ru–C(O) distances trans to the μ-PPh_2 are the longest, those trans to the Ru–Ru are intermediate in length, and those cis to the μ-PPh_2 are the shortest. In **8**, Ru–C2 and Ru–C3 represent the bonds to the bridging CO's and they are lengthened to 2.09 (2) and 2.10 (2) Å while there is virtually no distinction among the remaining Ru–C distances [1.86 (2)–1.90 (2) Å]. In both structures the Pt atom is involved in several C–H···Pt intramolecular contacts (3.01, 3.07, and 3.14 Å in **6b** and 3.03 Å in **8**), while the shortest intramolecular Pt···CO and Ru···CO contacts are Pt···C23 = 3.151 Å, Pt···C13 = 3.350 Å, and Ru2···C1 = 3.073 Å in **6b** and Pt···C2 = 3.424 Å, Pt···C3 = 3.472 Å, and Ru1···C1 = 3.014 Å in **8**. The shortest intermolecular contacts in 6b are O12···H215 = 2.47 Å, O13···H212 = 2.46 Å and H25···H224 = 2.19 Å and in **8** they are O2···H29 = 2.59 Å, O3···H212 = 2.34 Å, and C214···C215 = 3.498 Å, H14···H223 = 2.36 Å.

Discussion

Solution NMR Studies. ^1H and $^{31}P\{^1H\}$ NMR data for the $PtRu_2$ complexes **6a** and **6b** and the $PtRu_3$ complex **8** are given in Table I. All three complexes exhibit a hydridic resonance consisting of a 1:4:1 triplet of 1:1:1:1 quartets. The values of $^1J_{^{195}Pt-^1H}$ (ca. 550 Hz) and the low values of $^2J_{^{31}P-^1H}$ (ca. 10–18 Hz) are consistent with a bridging hydrido structure in which both the μ-PPh_2 and PR_3 ligand are oriented cis to the μ-hydride. The low values of $^2J_{^{195}Pt-^{31}P_\mu}$ (ca. 180–200 Hz) are consistent with the phosphido ligand bridging the two ruthenium atoms and the downfield shift ($\delta(P_\mu) \sim 155$ ppm) observed in **6a** and **6b** are typical for a μ-PPh_2 bridging a metal–metal bond.[23] Given the structural similarities of **6b** and **8**, it is not surprising that their NMR data (Table I) exhibit similar values. A noteworthy exception however is the very large downfield shift of P_μ of complex **8** ($\delta(P_\mu)$ = 387 ppm) which is 222 ppm further downfield than $\delta(P_\mu)$ of **6b**. Given the structural similarity of the environment of P_μ in **6b** and **8** (Figure 3), the very large variation in $\delta(P_\mu)$ is not easily rationalized.

The complex $Pt_2Ru_3(\mu\text{-}PPh_2)(\mu\text{-}H)(CO)_9(PCy_3)_2$ (**10**) is formulated as such on the basis of NMR data. The complex exhibits a hydridic resonance at −11.2 with $J_{^{195}Pt-^1H}$ of 555 Hz typical of a bridging hydride bonded to Pt and with small couplings to three ^{31}P nuclei. The $^{31}P\{^1H\}$ NMR spectrum of **10** exhibits three resonances. Two are assignable to non-equivalent PCy_3 ligands and exhibit both one-bond and two-bond couplings to ^{195}Pt (see Experimental Section). As with **8**, complex **10** exhibits a very large downfield shift of the P_μ nuclei ($\delta(P_\mu)$ = 391 ppm). Thus the NMR data of **10** indicate the presence of two "$Pt(PCy_3)$" units and considerable structural similarity between **8** and **10**. A possible structure of **10** is one in which a "$Pt(PCy_3)$" fragment has been added to the $PtRu_2$ face of **8** "opposite" to the μ-H and μ-PPh_2 groups. [An alternative possibility is that compound **10** is of the form $Pt_2Ru_2(\mu\text{-}PPh_2)(\mu\text{-}H)(CO)_7(PCy_3)_2$—a product of the reaction of $Pt(C_2H_4)_2(PCy_3)$ with $PtRu_2(\mu\text{-}PPh_2)(\mu\text{-}H)(CO)_7(PCy_3)$ (**6b**), in which the second "$Pt(PCy_3)$" fragment is in a position analogous to the "$Ru(CO)_2$" fragment disposed trans to the μ-PPh_2 in **8**.]

Comments Concerning the Mechanism(s) of Formation of $PtRu_2(\mu\text{-}PPh_2)(\mu\text{-}H)(CO)_7(PR_3)$ (6) and $PtRu_3(\mu\text{-}PPh_2)(\mu\text{-}H)(CO)_9(PCy_3)$ (8). The complexity of reaction products and the lack of any observable intermediates prior to the formation of **6** and **8** makes a mechanistic analysis of these reactions difficult. Heating **8** (refluxing CH_2Cl_2, 3 h) does *not* result in the formation of **6b**, suggesting that **8** is not a precursor to the products **6**. Cluster fragmentation is a frequently encountered feature of $Ru_3(CO)_{12}$ + ligand chemistry.[24] *Assuming* that the initial reaction of $Ru_3(CO)_{11}(PPh_2H)$ with $Pt(C_2H_4)(PPh_3)_2$ and $Pt(C_2H_4)_2(PCy_3)$ involves oxidative addition of the P–H bond across Pt [as is observed for $(OC)_xM(PPh_2H)$ systems], it follows that the initially formed phosphido-bridged species [e.g. $Ru_3(CO)_{11}(\mu\text{-}PPh_2)PtH(PPh_3)_2$] undergoes fragmentation [loss of "Ru-

(20) Farrugia, L. J.; Howard, J. A. K.; Mitrprachachon, P.; Stone, F. G. A.; Woodward, P. *J. Chem. Soc., Dalton Trans.* **1981**, 155.

(21) () Bars et al.[21b] have commented upon how in intramolecular dynamic processes in various Pt-containing clusters (e.g. $[PtRh_2(\mu\text{-}H)(\mu\text{-}CO)(PPh_3)(\eta\text{-}C_5Me_5)_2]BF_4$] the integrity of a $PtH(CO)(PPh_3)$ moiety is retained as rotation of the $Rh_2(\mu\text{-}CO)_2(\eta\text{-}C_5Me_5)_2$ fragment occurs about an axis through Pt and the mid point of the Rh=Rh unit. Likewise, isomerization of a tetrahedral $Os_3Pt(\mu\text{-}H)_2(\mu\text{-}CH_2)(CO)_{10}(PCy_3)$ cluster occurs by rotation of an integral $Pt(CO)(PCy_3)$ fragment about an axis perpendicular to the Os_3 plane. Calculations[21c] on similar systems have given some idea of the energy differences involved and have suggested that in PtL_2-capped M_3 clusters a structural alternative is for the PtL_2 plane to slip relative to the M_3 bonds as is observable in complex **8**. (b) Bars, O.; Braunstein, P.; Geoffroy, G. L.; Metz, B. *Organometallics* **1986**, *5*, 2021. (c) Schilling, B. E. R.; Hoffmann, R. *J. Am. Chem. Soc.* **1979**, *101*, *3456*.

(22) Favas, M. C.; Kepert, D. L. *Prog. Inorg. Chem.* **1980**, *27*, 325.

(23) (a) Carty, A. J. *Adv. Chem. Ser.* **1982**, *No. 196*, 1963. (b) Garrou, P. E. *Chem. Rev.* **1981**, *81*, 229.

(24) Brodie, N. M. H.; Chen, L.; Poe, A. J. *Int. J. Chem. Kinet.* **1988**, *20*, 467.

$(CO)_4$"] accompanied by μ-PPh_2 migration very rapidly. The nature of this process is not well understood. Similar μ-PPh_2 migration from an "MPt" site to an "M_2" site is also observed in the reaction of $Re_2(\mu\text{-}PPh_2)(\mu\text{-}H)(CO)_8$ with $Pt(C_2H_4)_2(PCy_3)$.[6] Likewise, in the iron–platinum system $FePt_2(\mu\text{-}PPh_2)(\mu\text{-}H)(\mu\text{-}CO)(CO)_3(PCy_3)_2$, the initially formed trimer contains a μ-PPh_2 bridging a "FePt" site. On standing, migration of the μ-PPh_2 ligand occurs to give an isomeric trimer in which the μ-PPh_2 bridges a "Pt_2" site.[5]

The formation of a mixture of **8** and **6b** from the reaction of $Ru_3(CO)_{11}(PPh_2H)$ (**4**) with $Pt(C_2H_4)_2(PCy_3)$ (eq 5) may reflect two very different reaction pathways. Oxidative addition of the P–H bond across Pt could be the initial step in the formation of **6b** while addition of a "$Pt(PCy_3)$ unit" across an "$Ru_2(CO)_2$" fragment of **4** could be the initial step in the formation of **8**. A similar proposal has been made to account for the observed difference in the reactions of $Pt(C_2H_4)_2(PCy_3)$ and $Pt(C_2H_4)(PPh_3)_2$ with $Re_2(CO)_9(PR_2H)$.[6] The possibility that formation of **6** and **8** from **4** occurs via initial formation of $Ru_3(\mu\text{-}PPh_2)(\mu\text{-}H)(CO)_{10}$ (**5**), which then reacts with the Pt complexes, can be excluded on the grounds that formation of **6** and **8** occurs more rapidly with **4** than the corresponding reaction with **5**.

Experimental Section

General Data. All manipulations were carried out under an atmosphere of dry N_2 using dry degassed solvents. Phosphorus and proton NMR spectra were recorded as CD_2Cl_2 solutions at room temperature on a Varian XL200 FTNMR spectrometer operating at 80.9 and 200 MHz, respectively. Proton shifts were measured relative to TMS. Phosphorus shifts were measured relative to external $P(OMe)_3$ in C_6D_6 and corrected to 85% H_3PO_4, with downfield shifts reported as positive. Infrared data were obtained on a Nicolet 10DX FTIR spectrometer. Samples were run as CH_2Cl_2 solution in sodium chloride cells.

Starting Materials. Deuteriodichloromethane was purchased from Aldrich and used as received. $Ru_3(CO)_{12}$ was purchased from Strem and used without further purification. Diphenylphosphine was purchased from Pressure Chemicals. The compounds $Ru_3(CO)_{11}(PPh_2H)$, $Ru_3(\mu\text{-}PPh_2)(\mu\text{-}H)(CO)_{10}$,[7] $Pt(C_2H_4)_2(PCy_3)$,[25] and $Pt(C_2H_4)(PPh_3)_2$[26] were prepared according to published procedures. All reactions were carried out in CH_2Cl_2 (IR monitoring) or CD_2Cl_2 (NMR monitoring).

Reaction of $Ru_3(CO)_{11}(PPh_2H)$ (4) with $Pt(C_2H_4)_2(PCy_3)$. To a CD_2Cl_2 (1 mL) solution of **4** (0.15 g, 0.19 mmol) was added $Pt(C_2H_4)_2(PCy_3)$ 0.14 g, 0.27 mmol). The solution immediately darkened (cherry red). $^{31}P\{^1H\}$ NMR spectra were recorded at various intervals over a period of 5 h. The reaction was repeated for ^1H NMR study.

Isolation of $PtRu_2(\mu\text{-}PPh_2)(\mu\text{-}H)(CO)_7(PCy_3)$ (6b). One of the above NMR samples was pumped to dryness, redissolved in the minimum amount of hexanes and allowed to stand at 0 °C for several days. Complex **6b** crystallized as yellow needles (0.025 g). IR (CH_2Cl_2, cm^{-1}): ν(CO) 2061 s (PtCO), 2029 vs, 2007 m, 1994 s, 1972 m, 1945 w.

Isolation of $PtRu_3(\mu\text{-}PPh_2)(\mu\text{-}H)(CO)_9(PCy_3)$ (8). One of the [**4** + $Pt(C_2H_4)_2(PCy_3)$] NMR samples was pumped to dryness. Recrystallization of the residue from CH_2Cl_2/MeOH yielded complex **8** as black prisms [together with minor amounts of yellow needles (**6b**)]. IR (CH_2Cl_2, cm^{-1}): ν(CO) 2054 m (PtCO), 2036 s, 2007 vs, 1976 m, 1959 m, 1862 w, br, 1809 m.

The reactions of **4** with $Pt(C_2H_4)(PPh_3)_2$ and **5** with $Pt(C_2H_4)_2(PCy_3)$ and $Pt(C_2H_4)_2(PPh_3)_2$ were similarly studied.

NMR Data of Identified Reaction Products [δ (ppm) and J (Hz)]. $Ru_3(\mu\text{-}PPh_2)(\mu\text{-}H)(CO)_{10}$ (**5**): $\delta(H) = -15.8$, $J^{31}P\text{–}^1H = 31$; $\delta(P) = 134.8$. $Pt_2Ru(CO)_5(PPh_3)_3$ (**7**): $\delta(PPh_3(Ru)) = 41$, $^2J_{^{195}Pt\text{–}^{31}P} = 81$, $J_{^{31}P\text{–}^{31}P} = 5$; $\delta(PPh_3(Pt)) = 54.5$, $^1J_{^{195}Pt\text{–}^{31}P} = 4733$, $^2J_{^{195}Pt\text{–}^{31}P} = 521$, $^4J_{^{31}P\text{–}^{31}P} = 58$, $^4J_{^{31}P(Ru)\text{–}^{31}P(Pt)} = 5$. $Pt_2Ru(CO)_6(PCy_3)_2$ (**9**) (tentative structural assignment): $\delta(P) = 63$, $^1J_{^{195}Pt\text{–}^{31}P} = 4451$, $^2J_{^{195}Pt\text{–}^{31}P} = 349$, $^4J_{^{31}P\text{–}^{31}P} = 43$. $Pt_3(CO)_3(PCy_3)_3$: $\delta(P) = 70.7$, $^1J_{^{195}Pt\text{–}^{31}P} = 4382$, $^2J_{^{195}Pt\text{–}^{31}P} = 411$, $^3J_{^{195}Pt\text{–}^{31}P} = 56$ (lit. values[27] 69.8, 4412, 430, 58). $Pt_2Ru_3(\mu\text{-}PPh_2)(\mu\text{-}H)(CO)_9(PCy_3)_2$ (**10**) (tentative structural assignment): $\delta(H) = -11.2$, $^1J_{^{195}Pt\text{–}^1H} = 555$, $J_{^{31}P\text{–}^1H} = 13, 8, 4$; $\delta(P_\mu) = 391$, $^2J_{^{195}Pt\text{–}^{31}P} = 224$, $J_{^{31}P\text{–}^{31}P} = 14.5, 12$. $\delta(PCy_3) = 72$, $^1J_{^{195}Pt\text{–}^{31}P} = 4528$, $^2J_{^{195}Pt\text{–}^{31}P} = 185$, $J_{^{31}P\text{–}^{31}P} = 14.5, 7$, $\delta(PCy_3) = 46.5$, $^1J_{^{195}Pt\text{–}^{31}P} = 3088$, $^2J_{^{195}Pt\text{–}^{31}P} = 79$, $J_{^{31}P\text{–}^{31}P} = 12, 7$.

X-ray Structure Determinations of 6 and 8. All work was performed on an Enraf-Nonius CAD4 diffractometer by the use of graphite-monochromatized Mo Kα radiation. All experimental details are given in Table II.

Acknowledgment. We thank the Natural Sciences and Engineering Research Council of Canada for financial support of this research.

Registry No. **4**, 87984-98-3; **5**, 80800-57-3; **6a**, 123263-89-8; **6b**, 123263-85-4; **7**, 34852-58-9; **8**, 123263-86-5; **9**, 123263-87-6; **10**, 123263-88-7; $Pt(C_2H_4)_2(PCy_3)$, 57158-83-5; $Pt_3(CO)_3(PCy_3)_3$, 62987-80-8; $Pt(C_2H_4)(PPh_3)_2$, 12120-15-9; $Pt(C_2H_4)_2(PH_3)_2$, 113155-47-8; $Ru_3(CO)_{12}$, 15243-33-1; Pt, 7440-06-4; Ru, 7440-18-8.

Supplementary Material Available: Tables of crystal data, intensity measurements, and structural refinements, atomic and thermal parameters, complete bond lengths and bond angles, and the results of a least-squares fit of the atoms of **8** to those of **6b** (37 pages); tables of final structure factor amplitudes for compounds **6b** and **8** (50 pages). Ordering information is given on any current masthead page.

(25) Spenser, J. L. *Inorg. Synth.* **1979**, *19*, 216.
(26) Blake, D. M.; Roundhill, D. M. *Inorg. Synth.* **1978**, *18*, 120.
(27) Moor, A.; Pregosin, P. S.; Venanzi, L. M. *Inorg. Chim. Acta* **1981**, *48*, 153.